Lessons Learned from Inlet Integration Analysis of NASA's Low Boom Flight Demonstrator

David Friedlander, Christopher Heath, and Ray Castner

NASA Glenn Research Center

10/25/17

Outline

- Background
- High Speed Wind Tunnel Test
- Numerical Modeling
- CFD Test Parameters
- Results
- Conclusions

Background

- In 2016, the NASA Aeronautics Research Mission Directorate announced the New Aviation Horizons Initiative with a goal of designing/building several x-planes, including a Low Boom Flight Demonstrator (LBFD).
- That same year, NASA awarded a contract to Lockheed Martin (LM) to advance the LBFD concept through preliminary design.
- Several configurations of the LBFD aircraft were analyzed by both LM engineers and NASA researchers.
- This presentation focuses on some of the CFD simulations that were run by the NASA Glenn Research Center (GRC) researchers.

An artist's concept of the LM LBFD preliminary design

High Speed Wind Tunnel Test

- A 9.5% scale vehicle configuration with integrated inlet, denoted C607.1, was tested in the NASA GRC 8'x6' Supersonic Wind Tunnel in April of 2017 to gather inlet performance data for comparison with CFD pre/post-dictions.

- The inlet was tested in freestream Mach numbers ranging from 0.3-1.56 at various alpha and beta angles.

- Three different set points were chosen for comparison with CFD:
  - Cruise point (Reading #1755)
  - Lower supersonic point (Reading #1771)
  - Subsonic point (Reading #2033)

Reading #	Mach Number*	Alpha (deg)*	Beta (deg)*
1755	1.455	1.994	0.00
1771	1.353	2.988	0.00
2033	0.2998	2.998	0.00

*Average values presented

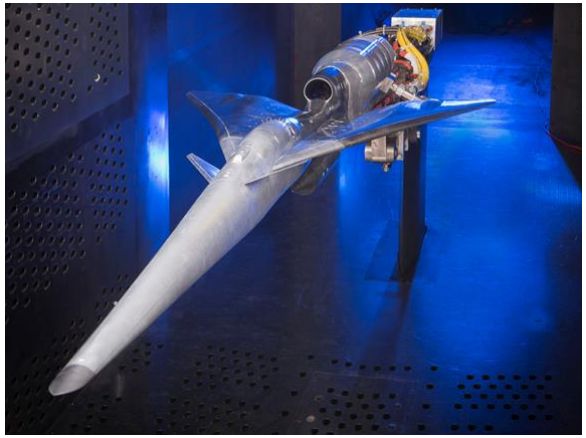

Numerical Modeling

- All powered inlet analyses were performed on the 9.5% scale C607.1 wind tunnel model.
- NASA's FUN3D v13.1 code was used for all adjoint-based grid refinement.
- The refine/one library was applied, which requires “freezing” all boundary layer cells within a user-specified distance from no-slip walls. In addition, only tetrahedral cells were modified during refinement. Pentahedral cells (prisms/pyramids) were left unchanged.
- The Spalart-Allmaras turbulence model was used during adaptation.

FUN3D

- Production code developed and maintained at the NASA Langley Research Center.
- Node-based, finite volume Navier-Stokes flow solver
- Can solve both incompressible and compressible flow problems on unstructured grids.

Adjoint-Based Grid Adaptation

- Adjoint-based grid adaptation has been effectively demonstrated in a number of cases to improve grid resolution near flow discontinuities and provide improved comparisons against experimental data.

- Past examples* include complex nozzle plume flows and problems in near-field sonic boom prediction.

- The adjoint process works by reducing the grid spatial discretization error w.r.t. a specified flow field metric (i.e. pressure within a region) by leveraging sensitivities in the flowfield.

- An adjoint-based grid adaptation study was performed to explore the sensitivity of the grid refinement process on various user-specified adaptation parameters.

*see adjoint-based grid adaptation references at end of slide package.

CFD Test Parameters

- A number of starting grids were generated using Pointwise/AFLR3 and subsequently adapted to understand how the refined solutions evolved from different initial conditions and with different adaptation parameters. Specifically:
  - Prism/pyramid vs. tetrahedral cells in the boundary-layer
  - Grid adaptation metric (engine axis-aligned linear pressure sensor vs. “pressure box” objective)
  - Rough vs. smooth transition from prisms to tetrahedrals permitted during adaptation
  - Total number of mesh adaptation cycles performed (16 vs. 8)

Effect of Boundary-Layer Cell Type

(Reading #1755, M=1.455)

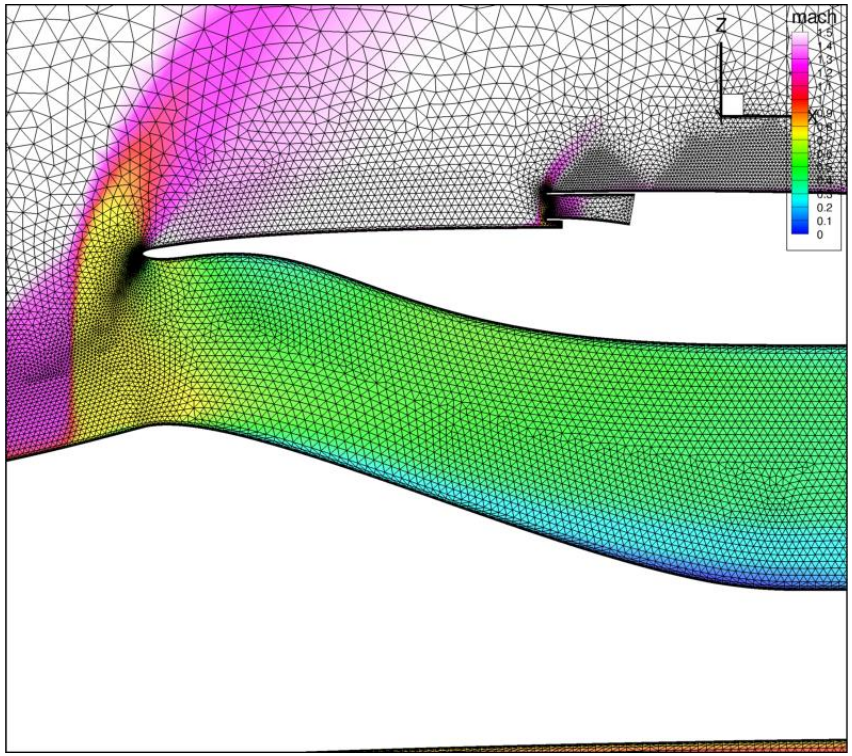

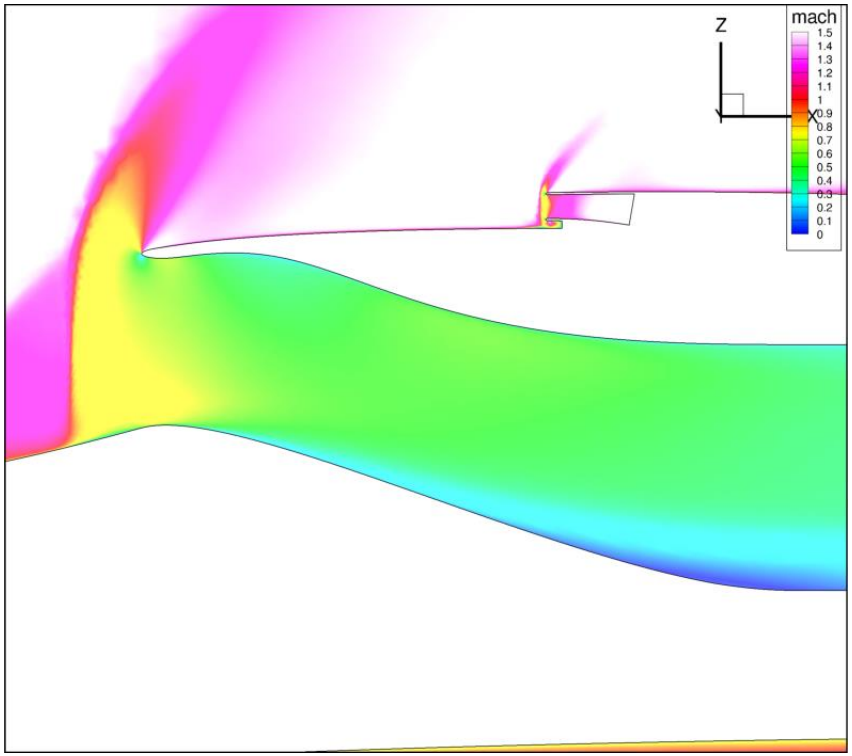

Coarse All Tetrahedral Case: "Coarse" initial grid, not adapted. Solution indicates marginal separation in the subsonic diffuser.

Effect of Boundary-Layer Cell Type

(Reading #1755, M=1.455)

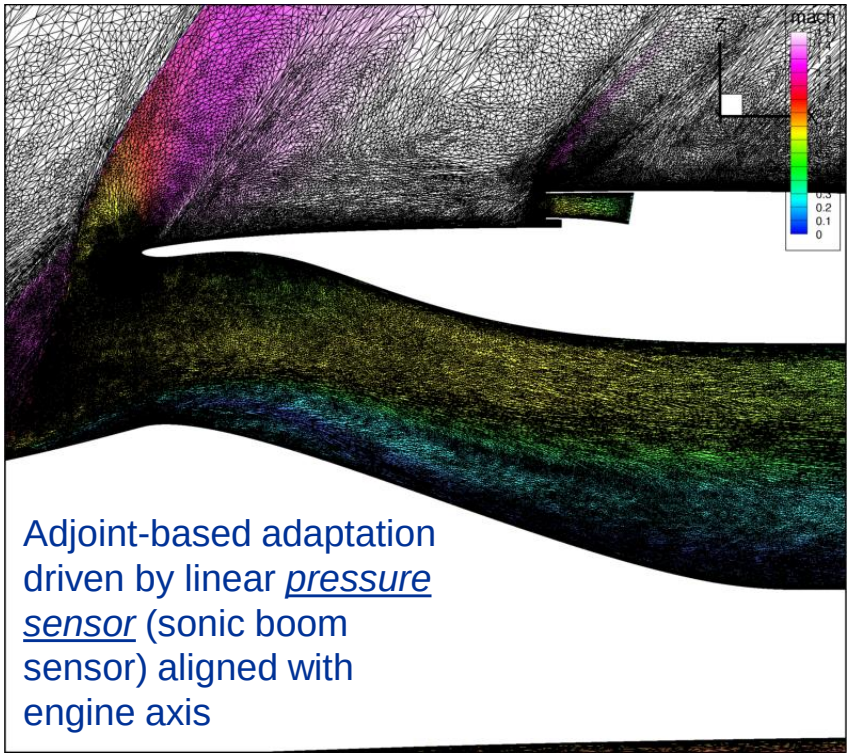

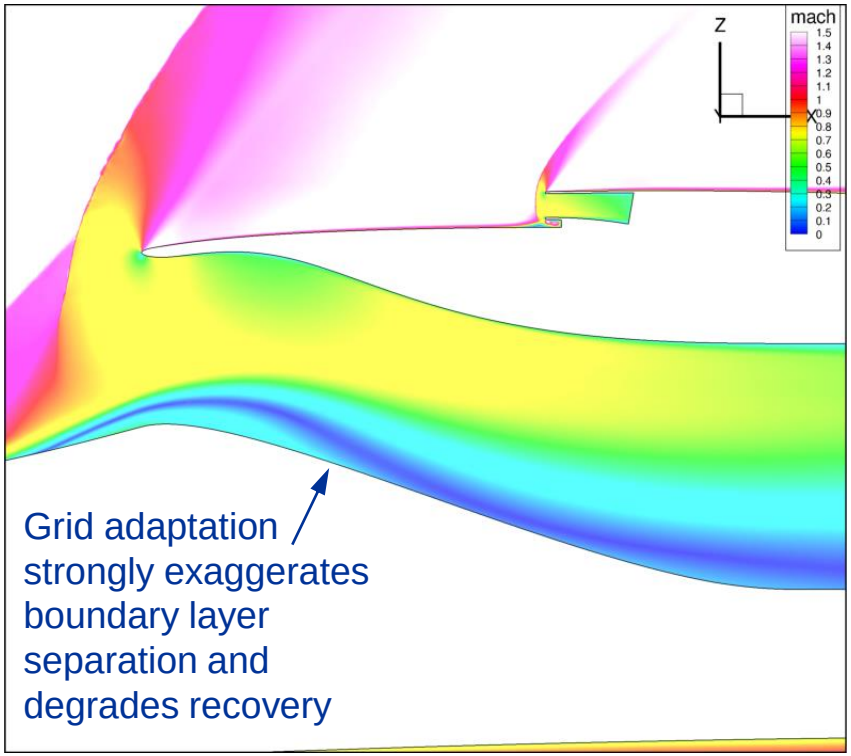

Refined All Tetrahedral Case: Grid refined 8 adaptation cycles using linear pressure sensor objective aligned with engine axis. Boundary layer cells frozen below y+ of ~300, permitting smooth grid transition from viscous layers.

Effect of Boundary-Layer Cell Type

(Reading #1755, M=1.455)

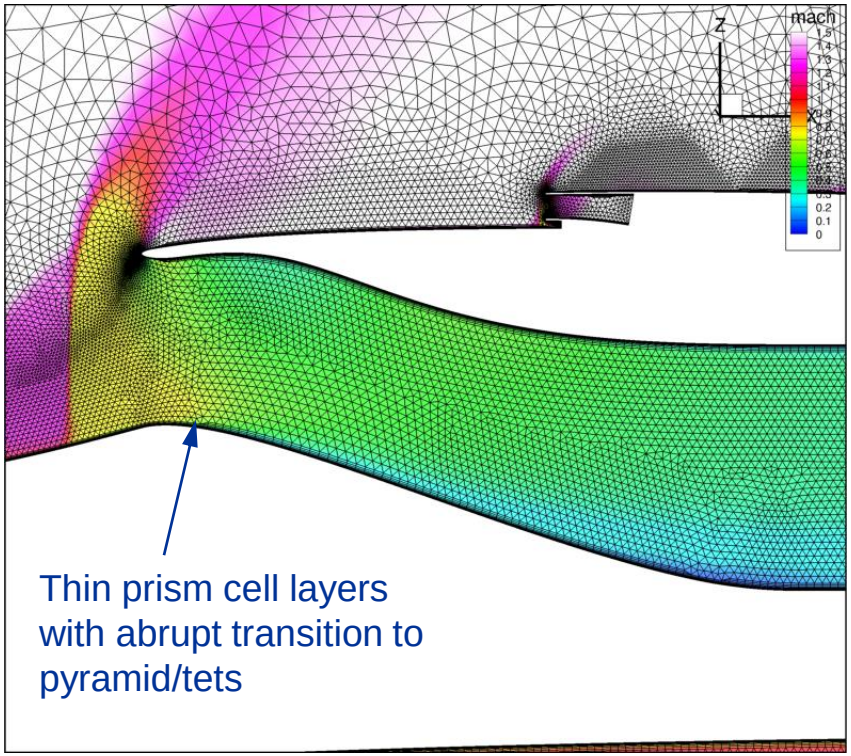

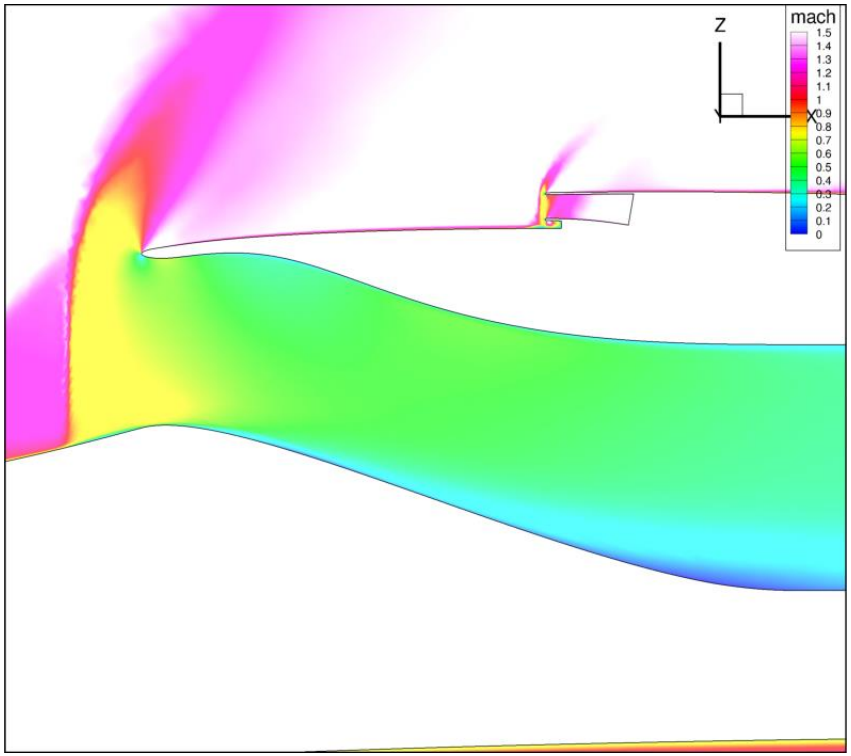

Coarse Pentahedral BL Case: “Coarse” grid with thin pentahedral boundary layer. Coarse grid solution again indicates marginal separation. More abrupt transition/termination of cells in the boundary layer.

Effect of Boundary-Layer Cell Type

(Reading #1755, M=1.455)

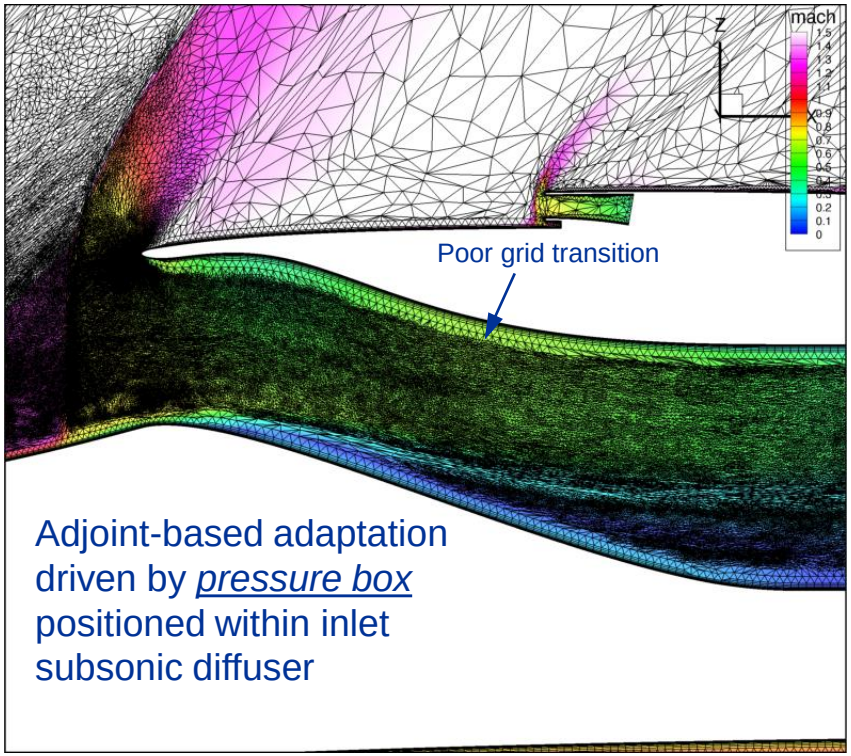

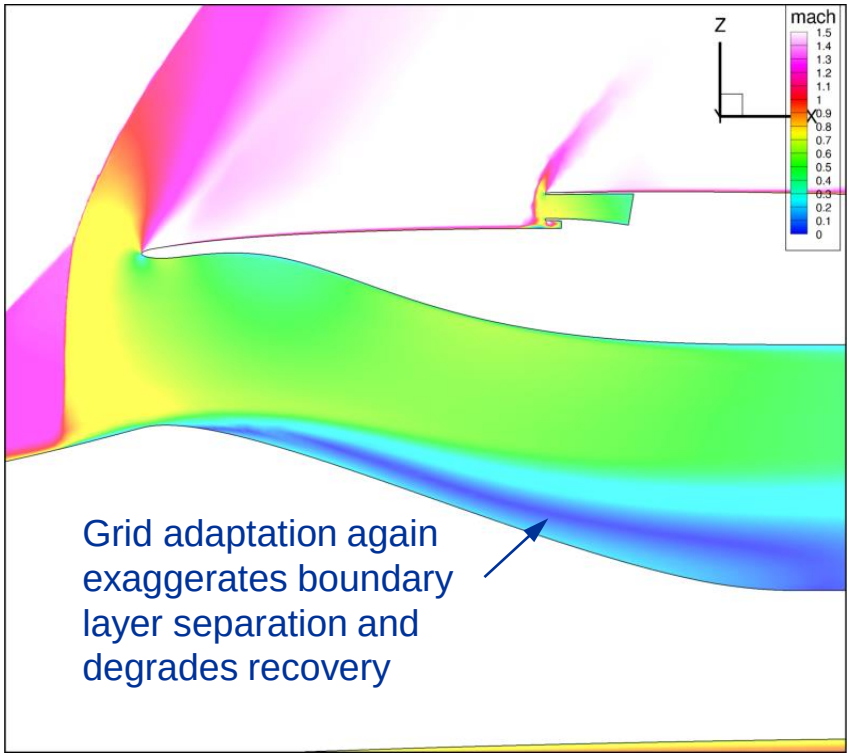

Refined Pentahedral BL Case: Adapted grid refined 8 adaptation cycles with thin pentahedral boundary layer and transition layer preserved. Results in poor grid transition from viscous layers near wall. Boundary layer cells of prism and pyramid types are “frozen”.

Effect of Boundary-Layer Cell Transition

(Reading #1755, M=1.455)

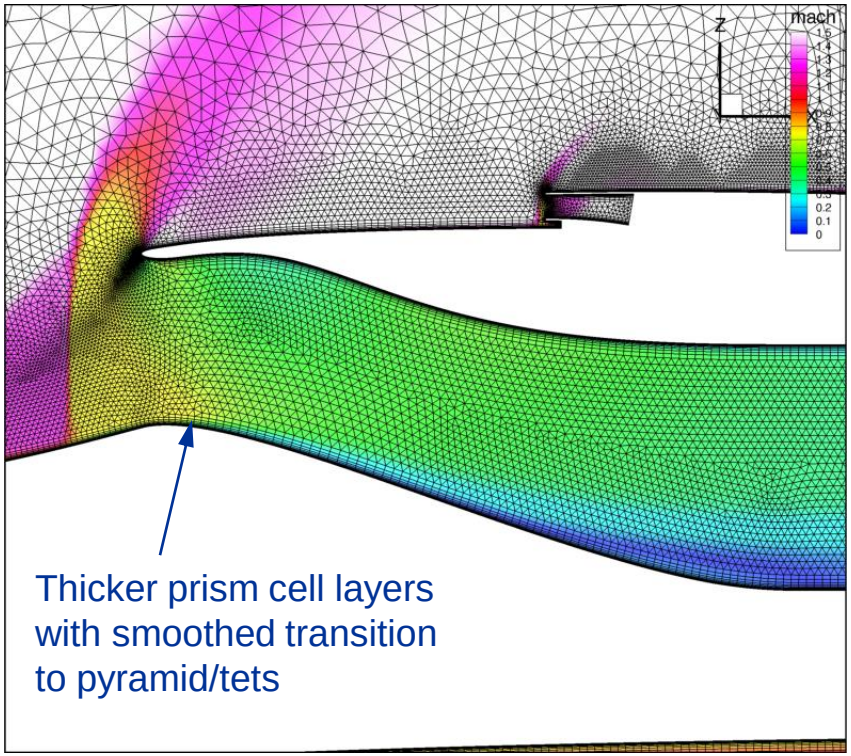

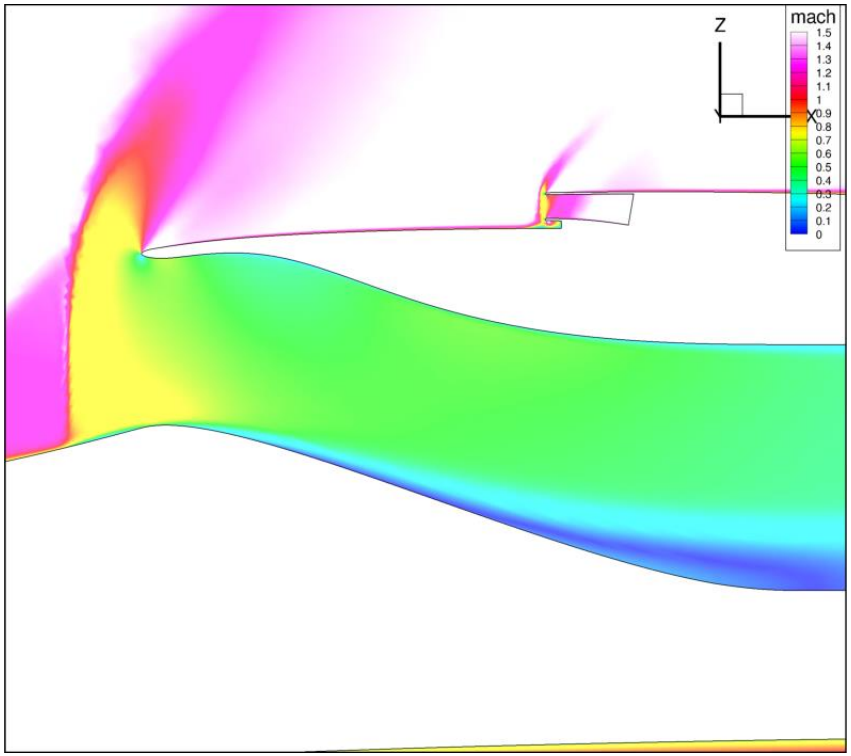

Coarse Smoothed Pentahedral BL Case: “Coarse” grid with thick pentahedral boundary layer and smooth BL transition. Yields slightly larger subsonic diffuser separation than previous coarse grid solutions.

Results (Reading #1755, M=1.455)

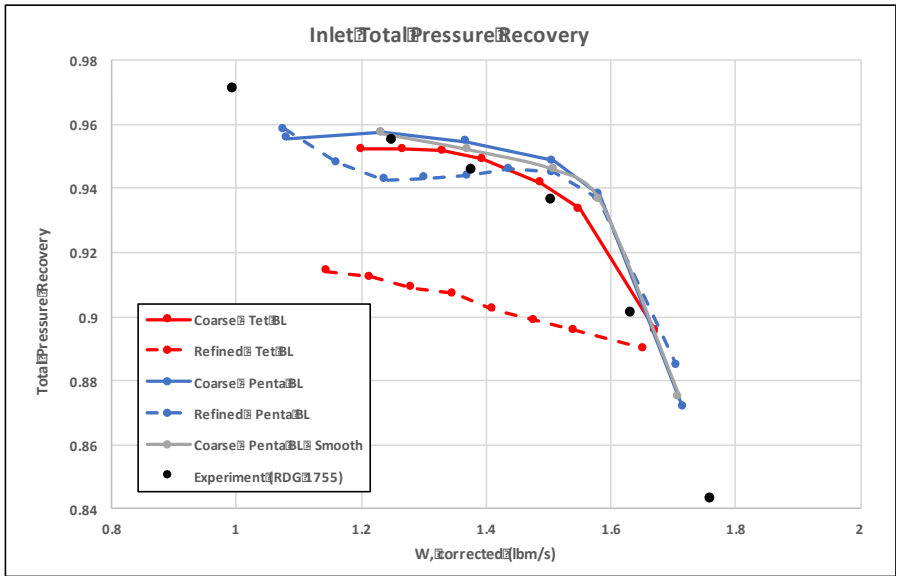

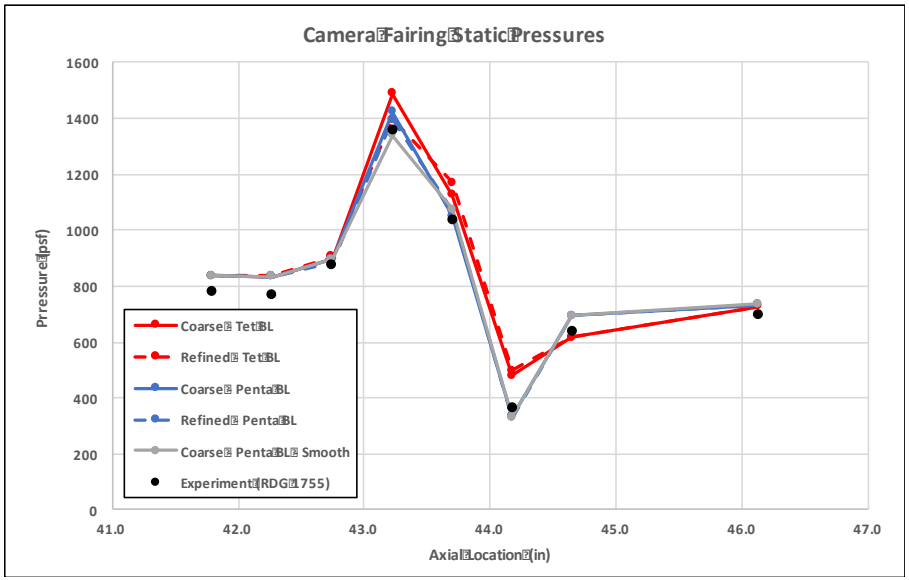

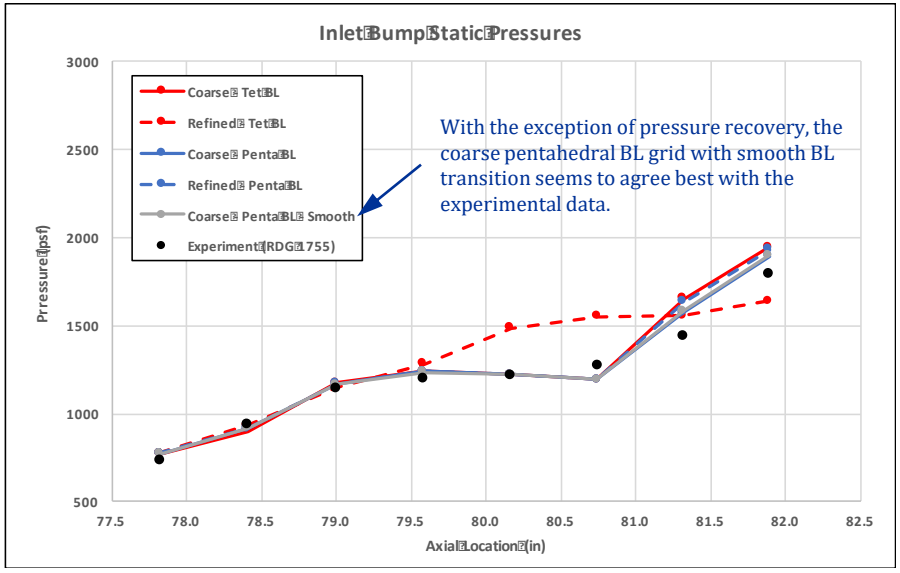

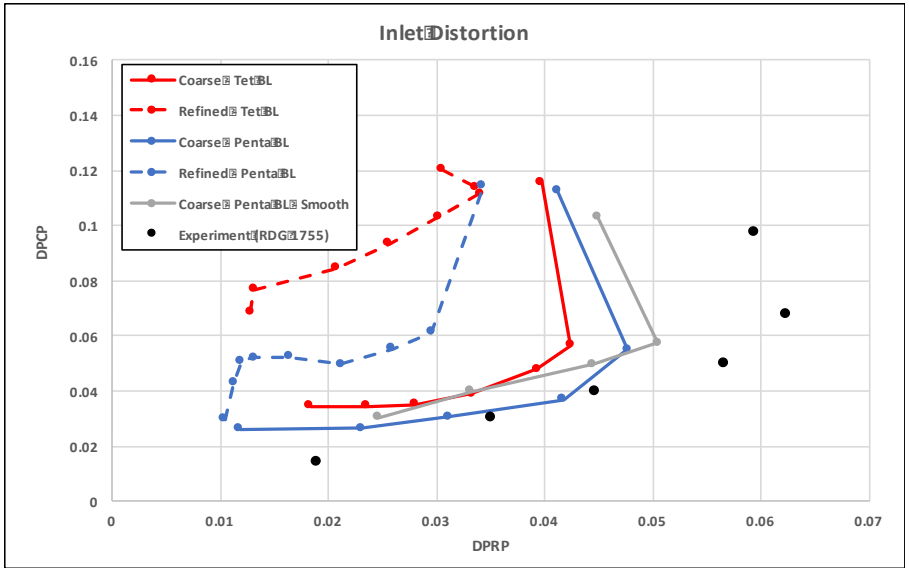

Effect of the Number of Grid Adaptation Cycles

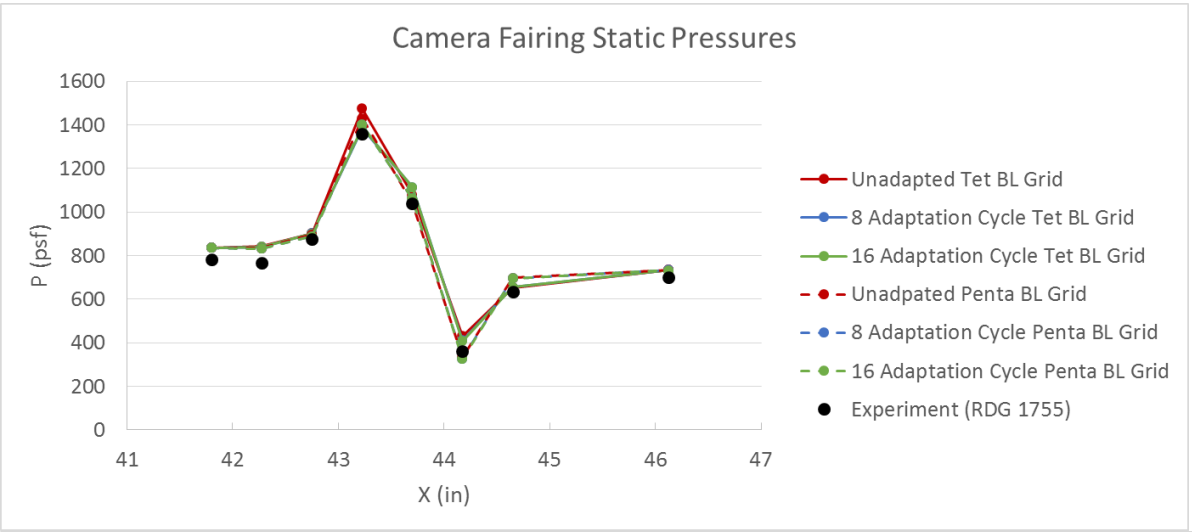

Camera Fairing:

- Pressure profiles tend to agree with each other.
- All solutions over-predict the first two upstream surface pressures.

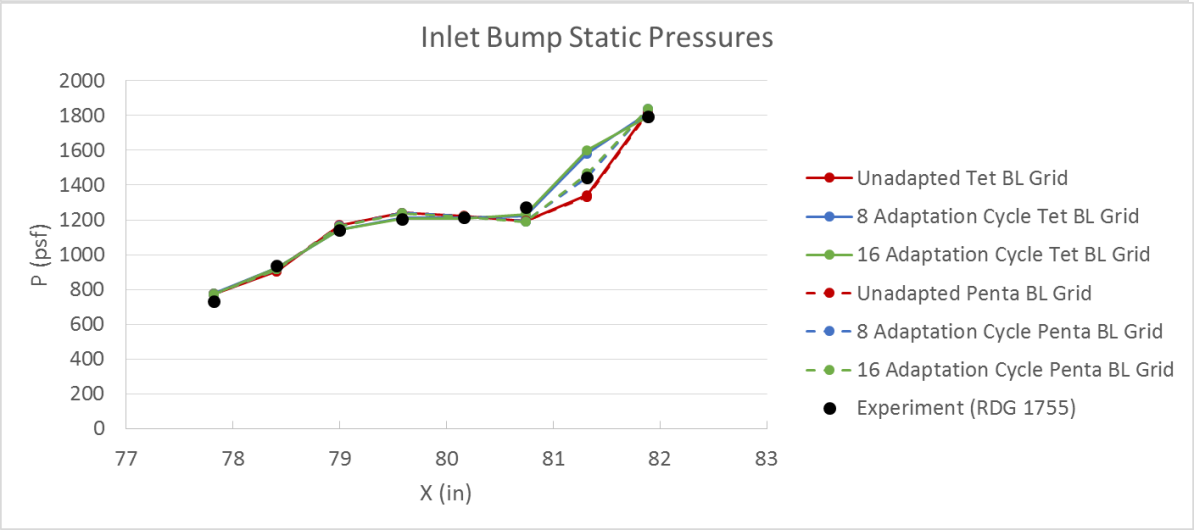

Inlet Bump:

- Pressure profiles agree with each other with the exception of the second to last downstream surface pressure.

Effect of the Number of Grid Adaptation Cycles

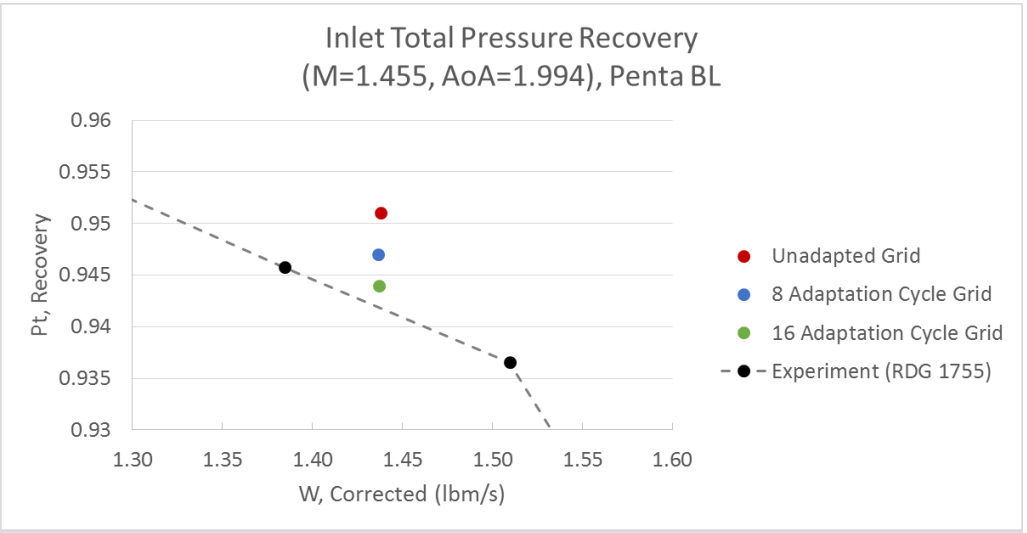

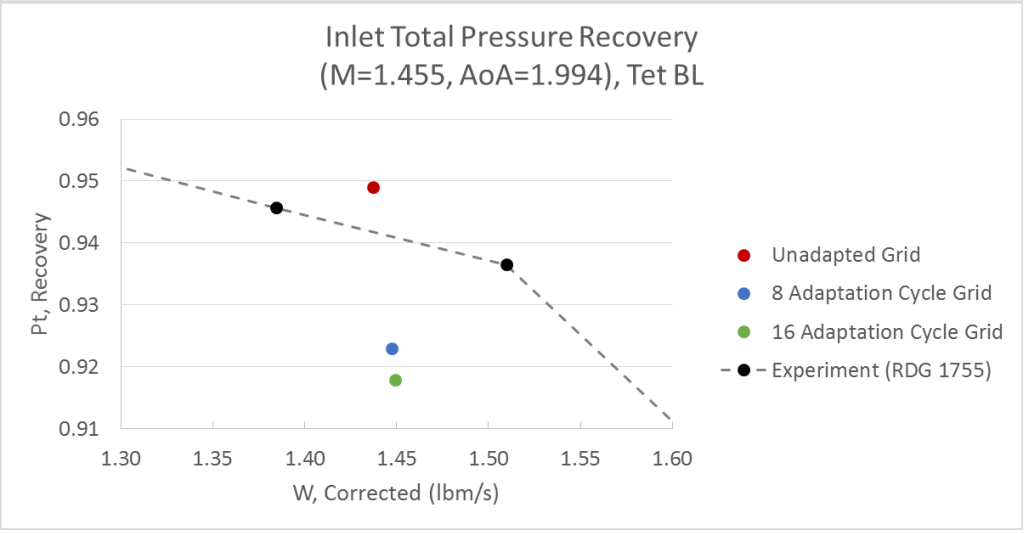

Computed total pressure recovery decreases asymptotically as the grid is further adapted. This is true for both the pentahedral BL and tetrahedral BL grids, however, the difference is most noticeable on the tetrahedral BL grid.

Reading #1771: Pressure Profiles

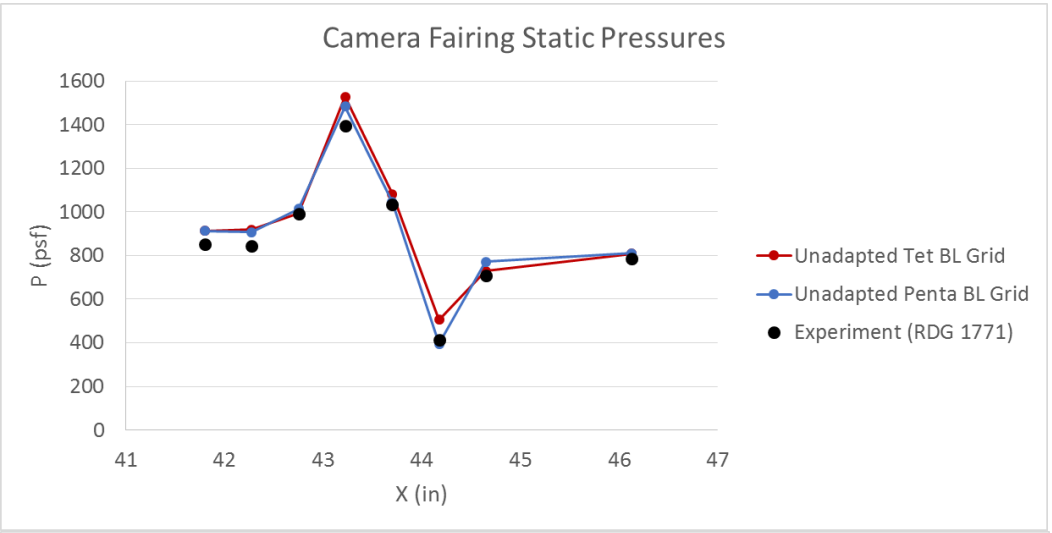

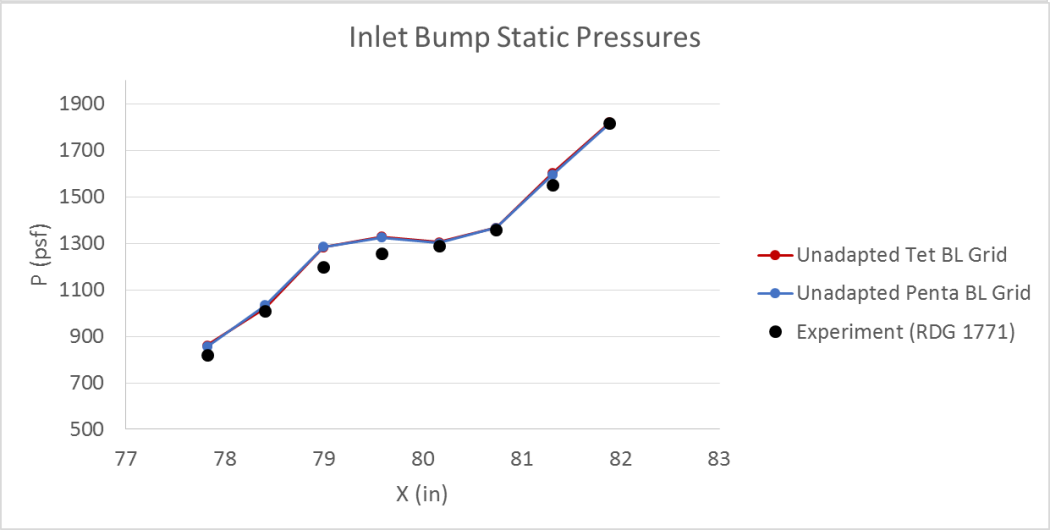

Camera Fairing:

- Pressure profiles tend to agree with each other.
- Both solutions over-predict the first two upstream pressure pressures.

Inlet Bump:

- Pressure profiles agree with each other.

Reading #1771: Total Pressure Recovery

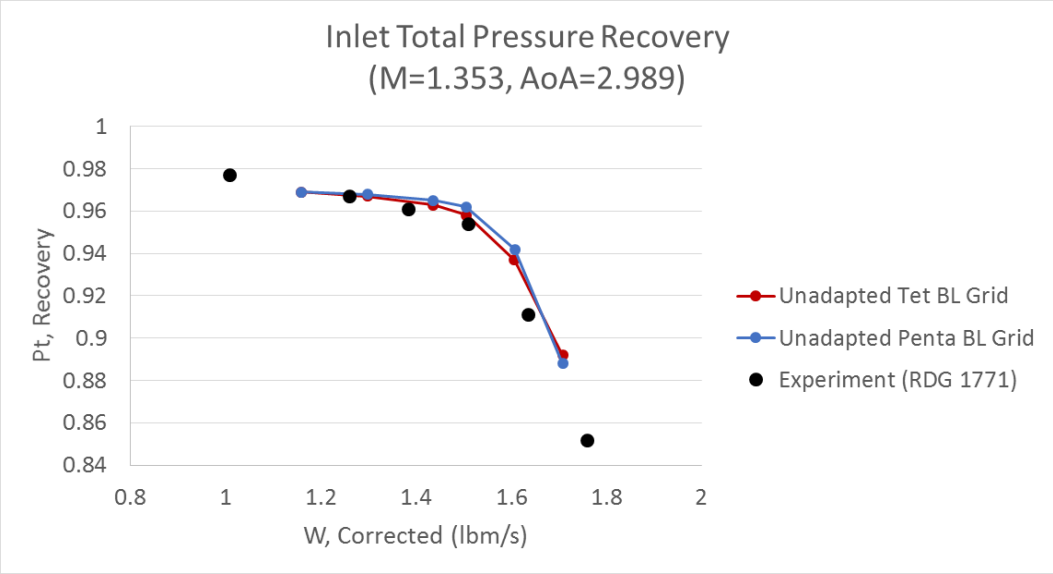

Both grids tend to compute the same total pressure recovery per corrected flow rate and agree well with experimental data.

Reading #2033: Pressure Profiles

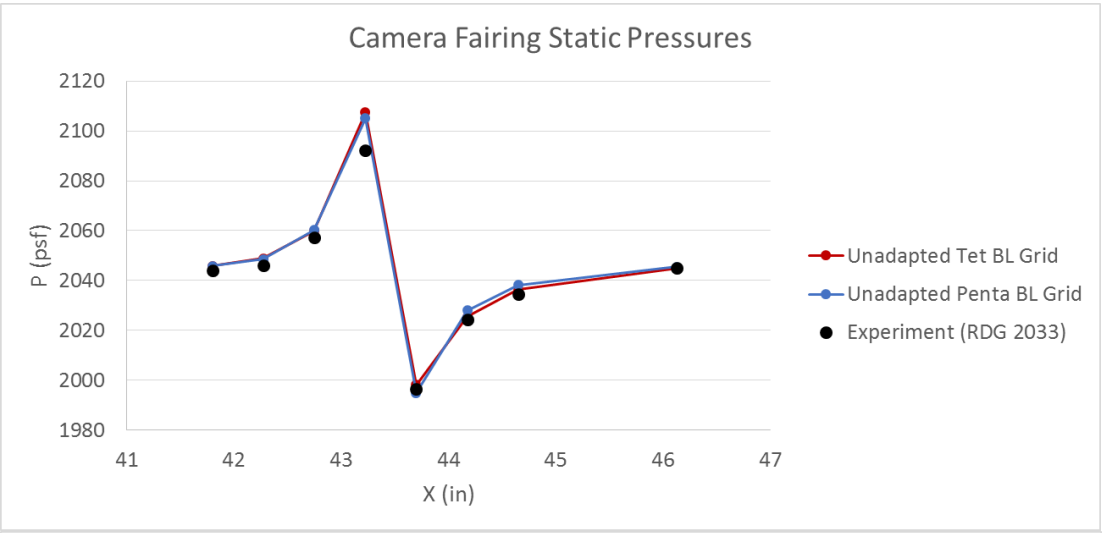

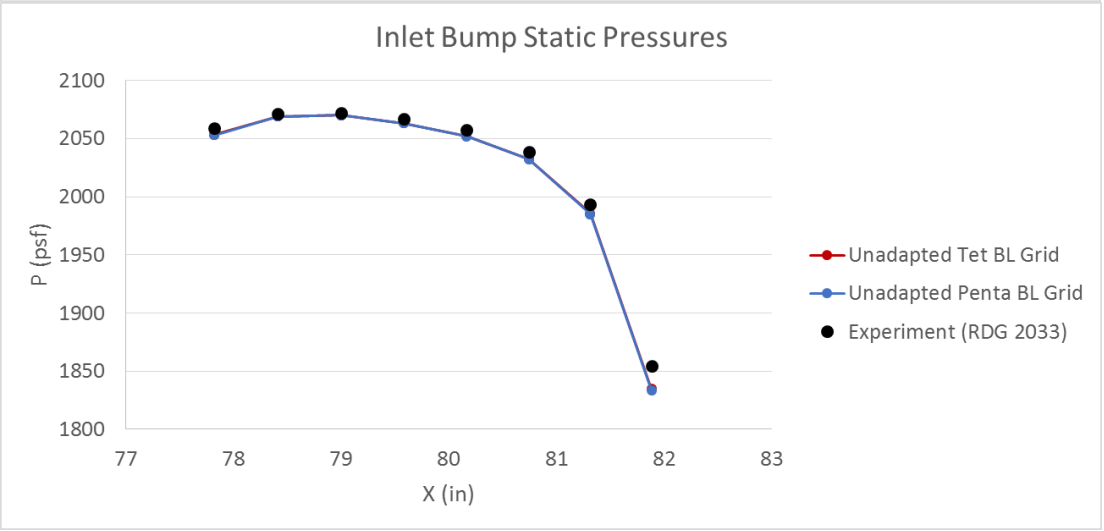

Pressure profiles agree with each other at both the camera fairing and the inlet bump.

Reading #2033: Total Pressure Recovery

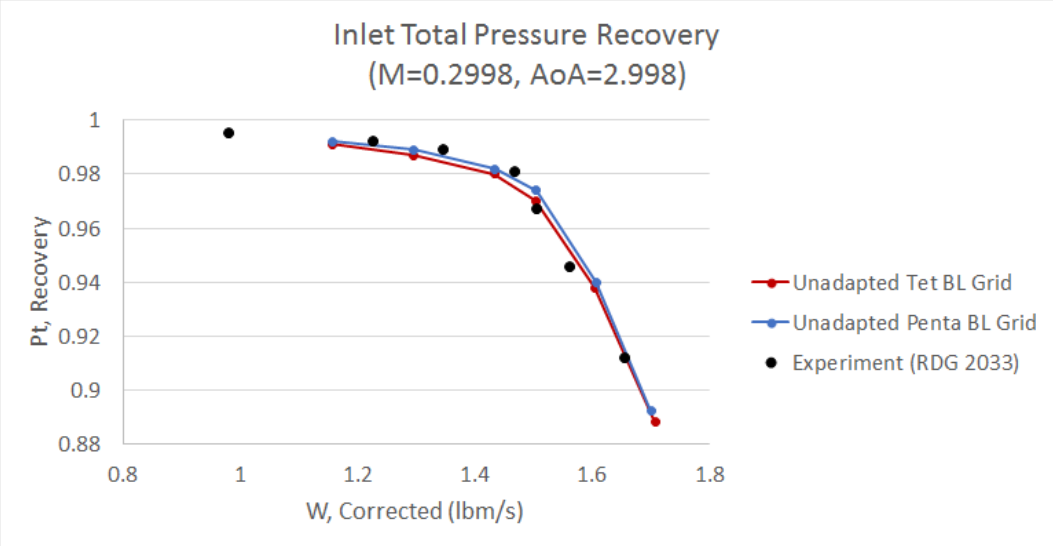

Both grids tend to compute the same total pressure recovery per corrected flow rate and agree well with experimental data.

Conclusions

- Prism/pyramid vs. tetrahedral cells in the boundary layer:
  - Prism/pyramid cells in the boundary layer generally perform better.
- Grid adaptation metric (engine axis-aligned linear pressure sensor vs. “pressure box” objective):
  - No significant difference between either adaption metric. Both produce similarly poor results.
- Rough vs. smooth transition from prisms to tetrahedrals:
  - Smooth transition of boundary layer elements is preferred.
- Total number of grid adaptation cycles performed:
  - Total pressure recovery decreases asymptotically as the number of grid adaptation cycles increases.

Adjoint-based grid adaptation did not accurately capture inlet performance for high speed top-aft-mounted propulsion.

Adjoint-Based Grid Adaptation References

- Alkandry, H., et. al., "Feature-Based and Output-Based Grid Adaptation Study for Hypersonic Propulsive Deceleration Jet Flows," 19th International Meshing Roundtable, Chattanooga, TN, October 2010.

- Park, M. A., and Darmofal, D. L., "Validation of an Output-Adaptive, Tetrahedral Cut-Cell Method for Sonic Boom Prediction," *AIAA Journal*, Vol. 48, No. 9, 2010, pp. 1928-1945.

- Bartels, R. E., et. al., "FUN3D Grid Refinement and Adaptation Studies for the Ares Launch Vehicle," AIAA-2010-4372, June 2010.

- Park, M. A., and Carlson, J.-R., "Turbulent Output-Based Anisotropic Adaptation," AIAA-2010-0168, January 2010.